Flexural stiffness of steel-concrete composite beam under positive moment

Fa-xing Ding [1], Jing Liu [*1], Xue-mei Liu [2], Feng-qi Guo [1] and Li-zhong Jiang [3]

[1] *School of Civil Engineering, Central South University, Changsha, Hunan Province, 410075, P. R. China.*

[2] *School of Civil Engineering and Built Environment, Queensland University of Technology, Brisbane, QLD 4000, Australia*

[3] *National Engineering Laboratory for High Speed Railway Construction, Changsha, 410075, P. R. China*

Abstract：This paper investigates the flexural stiffness of simply supported steel-concrete composite I-beams under positive bending moment through combined experimental, finite element (FE), and different standard analytical methods. .14 composite beams are tested for experimental study and parameters including shear connection degree, transverse and longitudinal reinforcement ratios, loading way are investigated. ABAQUS is employed to establish FE models to simulate the flexural behavior of composite beams. The influences of a few key parameters, such as the shear connection degree, stud arrangement, stud diameter, beam length, loading way, on the flexural stiffness are studied. In addition, three widely used standard methods including GB, AISC, and British standards are used to estimate the flexural stiffness of the composite beams. The results are compared with the experimental and numerical results. The results indicate that GB 50017-2003 could provide better estimation in comparison to the other standards.

Key words: steel-concrete composite beam; flexural stiffness; finite element; degree of shear connection

1. Introduction

Steel-concrete composite beams are a form of beam that efficiently utilize both concrete and steel materials with the concrete slabs resting upon steel beams, both bonded together by shear connectors to prevent separation or relative slip between the concrete slab and the steel beam. Such composite beams have been widely used for multi-story buildings and bridges. Deflection being a control parameter due to great span-depth ratio is always used in engineering, which is particularly important to predict the elastic deflection of composite beams under service load. Various standards are available to estimate the flexural stiffness of steel-concrete composite beams currently. Some of the standards have taken account of the slip effects into the calculation of flexure stiffness of the composite beams, while the others have not.

Nie *et al.*(2003) investigated the effects of shear slip on the deformation of steel-concrete composite beams, and a general formula to account for slip effects was developed, such proposal

*Corresponding author, Ph.D., E-mail: liujing001@csu.edu.cn

was accept and adopted by GB 50017-2003, AISC-LRFD specifies a reduced effective moment of inertia to account for slip in partial composite sections. Eurocode 4.2004 did not put forward a formula for computing the deflection of steel-concrete composite beams, however, a simplified calculation method was given by British standard BS5950-3.1. The slip effects were ignored for full composite sections according to AISC-LRFD and BS5950-3.1, which means composite beam can be considered with a fully composite uncracked transformed section.

The shear connection of steel-concrete composite beam can be divided into full shear connection and partial shear connection in theory. The former can minimize the deflection of composite beams under load, and guarantee the bearing capacity. The latter reduces the number of the stud and benefits reinforcing bar colligation, which is conducive to improve the ductility of composite beams in a certain extent and control concrete crack in the negative moment region at the same time. Because of the finite rigidity of those connectors which combined the steel and concrete parts to work together, longitudinal slips will occur at the interface between the two materials, the actual stiffness of beams with full composite design is about 80% of their calculated stiffness where slip is ignored under service load (Nie *et al*.2003).

Researchers have carried out extensive research on steel-concrete composite beam in theoretical and experimental research. Salari (1999) researched the bond-slip in steel-concrete composite beam, and presented three different composite beam elements to accounting the bond-slip effect. Zhao *et al*.(2012) have completed four full scale composite beams tests under monotonic positive and negative bending. Souici *et al*.(2013) researched the behaviour of steel-concrete composite beams with shear connection realised by means of either the traditional welded-studs or an innovative bonded solution based. Nie *et al*.(2011) conducted a loading capacity analysis for prestressed continuous steel-concrete composite beams. Hou *et al*.(2015) concerned with the dynamic analysis of simply-supported steel-concrete composite beams under moving loads. Selçuk *et al*.(2013) investigated bending behavior of reinforced concrete slabs encased over shallow I-sections at different levels of compression heads. Lezgy *et al*.(2015) used a refined high-order beam theory to Analysis of composite steel-concrete beams.

With the advancement of computing techniques and for the sake for saving time and cost, researchers tend to use more comprehensive method such as finite element analysis (FEA) to analyze the composite structural systems with validated FE models. Mirza *et al*.(2011) investigated the performance of beam-column flush end-plate connections when using blind bolts by ABAQUS. Sang-Hyo Kim *et al*.(2011) researched experimental and analytical evaluations of the degree of shear connection affected by stud diameter. Dias *et al*.(2015) applied a finite element computer code to study long-term behavior of steel-concrete composite structures under service loads.

This paper aims to thoroughly investigate the flexural stiffness of steel-concrete composite beams. To compare and evaluate different standard which applied in flexural stiffness calculation

of steel-concrete composite beam, and analyze those various parameters in a wider range. More specifically, based on the theoretical, FE application and experimental research in our team (Ding *et al.* 2011, Ding *et al.* 2015, Ding *et al.* 2016a; 2016b). four objectives are included in this study: (1) To investigate the flexural stiffness of 14 simply supported steel-concrete composite I-beam subjected to positive bending moment through experimental study; (2) To establish FE models using ABAQUS program to simulate the flexural performance of the steel-concrete composite beams; (3) To conduct parametric study to investigate the effect of degree of shear connection, stud arrangement, diameter of the stud, beam span, and loading condition on the flexural behavior of steel-concrete composite beams; (4) To compare and evaluate different standard methods including GB 50017, AISC-LRFD and BS5950-3.1 to the experimental results and numerical results from FEA on the flexural performance of steel-concrete composite beams.

2. Experimental study

2.1 Materials and specimens

14 steel-concrete composite beams were included into the experimental study. Cross section of girder is shown in Fig.1. Test loading device is shown in Figs.2-3. Detailed geometric properties and characteristics of the specimens are presented in Table 1. l is the length of the specimen, w_c is the width of the concrete slab, h_c is the depth of concrete, h_s is the height of steel beam and d is the diameter of stud. ρ_{st} is ratio of transverse reinforcement of concrete slab, ρ_{sl} is ratio of longitudinal reinforcement of concrete slab. η is the degree of shear connection (GB 50017). n_{all} is the number of shear connectors. p_1 is the longitudinal spacing of shear studs. For the convenience of calculation and analysis, parameters related to the specimens in literatures (Salari 1999, Nie *et al.*2003, Zhao *et al.*2012 and Souice *et al.*2013), are also given in Table 1.

Before the beam testing, material testing was conducted to obtain the respective material properties. The cubic compressive strength f_{cu} of concrete and tensile coupon tests on steel plates are presented in Table 2. f_y means the yield strength of steel, f_s means the yield strength of stud and f_{cu} represents the concrete compressive strength. Young's modulus of concrete E_c is $9500 f_{cu}^{1/3}$, which was suggested by Ding *et al.*(2011).
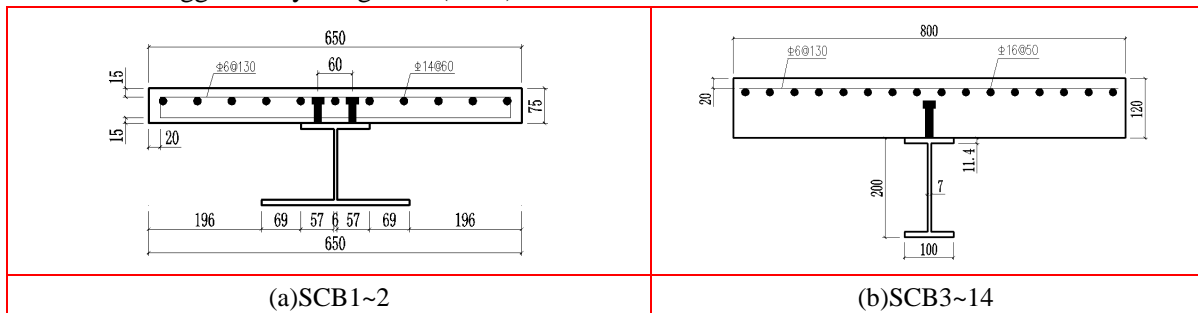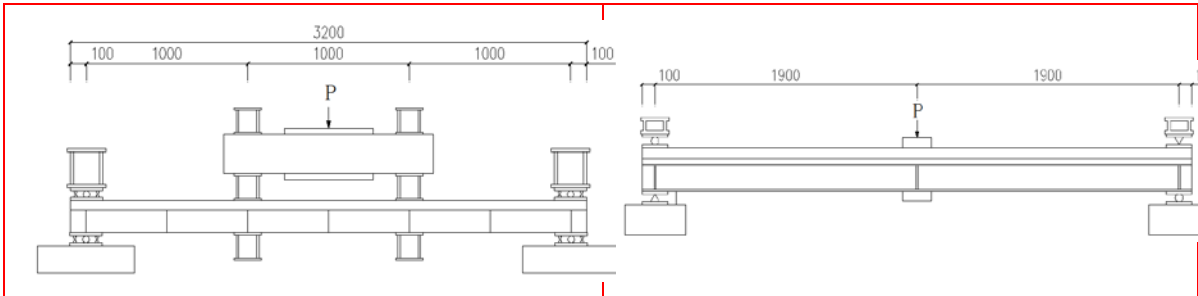

| (a)SCB1~2 | (b)SCB3~14 |

Fig.1 Cross section of girder

Fig.2 Experimental setup on spot

(a)SCB1~2	(b)SCB3~14

Fig.3 Experimental setup for all specimens

Table 1 Geometric properties and characteristics of composite beams

Source of the specimens	No.	Loading mode	l/mm	w_c/mm	h_c/mm	h_s/mm	d/mm	η	ρ_{st}/%	ρ_{sl}/%	p_1/mm	n_{all}	EI/10^7 N.m^2	(EI)/ $(EI)_2$	(EI)/ $(EI)_3$	(EI)/ $(EI)_4$
this paper	SCB1	dynamic cyclic	3000	650	75	140	13	0.85	0.62	3.47	75	78	0.74	1.12	0.74	0.74
	SCB2	dynamic cyclic	3000	650	75	140	13	0.34	0.62	3.47	200	30	0.80	0.05	1.07	1.38
	SCB3	dynamic cyclic	3800	800	120	200	16	1.86	0.32	2.51	65	62	1.94	0.97	0.75	0.75
	SCB4	dynamic cyclic	3800	800	120	200	16	1.62	0.32	2.51	75	54	1.76	0.90	0.68	0.68
	SCB5	dynamic cyclic	3800	800	120	200	16	1.32	0.32	2.51	90	44	1.68	0.88	0.65	0.65
	SCB6	dynamic cyclic	3800	800	120	200	16	1.08	0.32	2.51	110	36	1.66	0.90	0.64	0.64
	SCB7	dynamic cyclic	3800	800	120	200	16	0.84	0.32	2.51	140	28	1.64	0.90	0.63	0.63
	SCB8	monotolic	3800	800	120	200	16	1.32	0.32	3.35	90	44	1.77	0.90	0.66	0.66
	SCB9	monotolic	3800	800	120	200	16	1.32	0.32	2.93	90	44	1.73	0.89	0.66	0.66
	SCB10	dynamic cyclic	3800	800	120	200	16	1.32	0.20	2.51	90	44	2.20	1.16	0.85	0.85
	SCB11	dynamic cyclic	3800	800	120	200	16	1.32	0.43	2.51	90	44	1.98	1.04	0.77	0.77
	SCB12	dynamic cyclic	3800	800	120	200	16	1.32	0.59	2.51	90	44	2.17	1.14	0.84	0.84

	SCB13	dynamic cyclic	3800	800	120	200	16	1.32	0.78	2.51	90	44	2.22	1.17	0.86	0.86
	SCB14	dynamic cyclic	3800	800	120	200	16	1.32	1.18	2.51	90	44	2.23	1.17	0.86	0.86
Salai 1999	SC1	monotolic	5490	1220	152	305	13	0.83	0.20	0.21	55	100	1.73	0.91	0.78	0.78
Nie *et al.* 2003	CB1	monotolic	3840	500	125	200	19	1.12	0.62	0.63	115	34	1.48	0.81	0.60	0.60
	CB2	monotolic	3840	800	125	200	19	1.12	0.62	0.40	115	34	1.61	0.87	0.63	0.63
	CB3	monotolic	3840	800	125	200	19	1.02	0.62	1.55	148	26	1.46	0.77	0.56	0.56
	CB4	monotolic	3840	800	125	200	19	1.02	0.62	2.01	148	26	9.53	1.21	0.87	0.87
Zhao *et al.* 2012	SCB1	monotolic	4000	600	100	150	16	1.10	1.73	1.04	190	46	0.88	0.84	0.64	0.64
	SCB2	monotolic	4000	600	100	150	16	1.67	2.45	1.04	125	70	0.87	0.78	0.64	0.64
Souici *et al.* 2013	B1	monotolic	3250	350	55	200	9	0.73	0.34	/	180	18	0.64	1.00	0.74	0.76
	B2	monotolic	3250	350	55	200	9	0.57	0.34	/	235	14	0.66	1.00	0.80	0.84
	B3	monotolic	3250	350	55	200	9	0.33	0.34	/	410	8	0.71	1.12	0.74	0.74

Table 2 Properties of steel and concrete

Source of the specimens	No.	f_{cu}/MPa	f_y/MPa	f_s/MPa	E_s/MPa
this paper	SCB1	35.5	311	330	$2.07×10^5$
	SCB2	35.5	311	330	$2.07×10^5$
	SCB3	44.3	250	350	$2.09×10^5$
	SCB4	44.3	250	350	$2.09×10^5$
	SCB5	48.5	250	350	$2.09×10^5$
	SCB6	42.2	250	350	$2.09×10^5$
	SCB7	43.4	250	350	$2.09×10^5$
	SCB8	38.2	250	350	$2.09×10^5$
	SCB9	46.2	250	350	$2.09×10^5$
	SCB10	41.9	320	350	$2.\,02×10^5$
	SCB11	42.1	320	350	$2.02×10^5$
	SCB12	49.7	320	350	$2.02×10^5$
	SCB13	40.8	320	350	$2.02×10^5$
	SCB14	45.1	320	350	$2.02×10^5$
Salai 1999	SC1	50.0	262	320	$2.02×10^5$
Nie *et al.* 2003	CB1	32.0	310	323	$2.03×10^5$
	CB2	32.0	310	323	$2.03×10^5$
	CB3	32.0	310	323	$2.03×10^5$
	CB4	32.0	310	323	$2.03×10^5$
Zhao *et al.*	SCB1	34.4	338	350	$2.00×10^5$

2012	SCB2	35.2	338	350	2.00×10^5
Souici *et al.* 2013	B1	35	235	355	2.10×10^5
	B2	35	235	355	2.10×10^5
	B3	35	235	355	2.10×10^5

2.2 Testing system and method

Experiments on steel-concrete composite beams specimens were conducted in the National Engineering Laboratory for High Speed Railway Construction. 14 specimens were designed and tested in two scenarios. The first scenario used the monotonic loading mode and included two specimens labeled SCB8 and SCB9. The second scenario applied dynamic cyclic loading mode and included the remaining 12 specimens for testing. In addition, four micrometer to measure slip between steel girder and concrete plate were installed, for specimens SCB1 and SCB2, which along the beam length on the beam fulcrum, 1/3, 1/6 of beam span and mid-span, sliding measuring points arrangement are shown in Fig.4.

Five displacement meters were installed, for specimens SCB1 and SCB2, which along the beam length on the beam of two fulcrum, 1/3, 2/3 of beam span and mid-span. Fig.5 shows steel-concrete composite beam deflection layout.

The flexural stiffness could be obtained from the load deflection curves under monotonic loading, while under dynamic cyclic loading the flexural stiffness was attained as the secant stiffness at 0.4 times of the ultimate load using the envelop curve.

Steel-concrete composite beams flexural stiffness and flexural rigidity of transformed section relationship is defined by:

$$(EI) = \theta(E_s I_{tr}) \tag{1}$$

where (EI) is the measured flexural stiffness of steel-concrete composite beams, θ is the flexural stiffness coefficient, $(E_s I_{tr})$ is flexural stiffness of transformed section, I_{tr} is the moment of inertia for the fully composite uncracked transformed section. We put the concrete flange plate of the composite beam into the steel ones according to the elastic modulus ratio and keep the thickness of section unchanged, as a result, get a equivalent section.
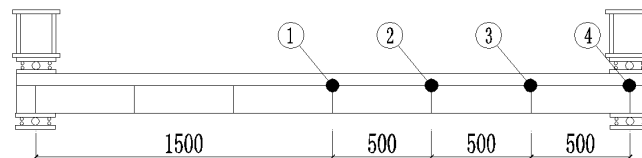

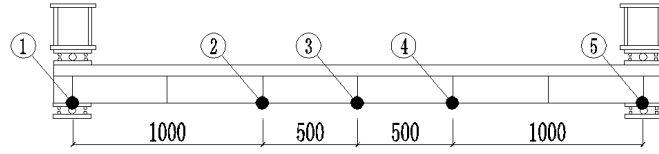Fig.4 Slip measuring points arrangement of steel-concrete composite beam

Fig.5 Steel-concrete composite beam deflection layout

2.3 Experimental results and discussion

To further understand the factors influencing the flexural stiffness of composite beams, this section focus on such factors with the following contents. In addition, the effect of the degree of shear connection on slip values and deflection curves are also discussed.

2.3.1 Factors influencing the flexural stiffness

(1) The degree of shear connection

Relationship between stiffness coefficient and degree of shear connection are shown in Fig.6. The contrast of SCB3~SCB7 shows that the greater the degree of shear connection, the larger the flexural stiffness. When η is greater than 1, the measured flexural stiffness of steel-concrete composite beams is smaller than that of the transformed section.

(2) The ratio of transverse reinforcement

Fig.7 illustrates the relationship between the ratio of transverse reinforcement and stiffness coefficient. The contrast of SCB10~SCB14 shows that the transverse reinforcement ratio between 0.20%~1.18%, θ of each specimen has not been affected by ρ_{st} regularly.

(3) The loading condition

The comparison of SCB7, SCB8 and SCB9 demonstrates that there is marginal difference in the flexural stiffness obtained from dynamic cyclic loading condition and monotonic loading condition with the same degree of shear connection. The flexural stiffness of SCB8 is 5.7% higher than that of the SCB7 specimen, and the flexural stiffness of SCB9 is only 2.9% higher than the SCB7 specimen, as shown in the Table 1. Such findings indicate that the flexural stiffness of composite beam obtained under monotonic loading condition is comparable to that obtained under dynamic cyclic loading condition. This suggests the flexural stiffness of the composite beam can be obtained through either monotonic or cyclic loading methods and the stiffness is generally the same obtained by using both loading method.
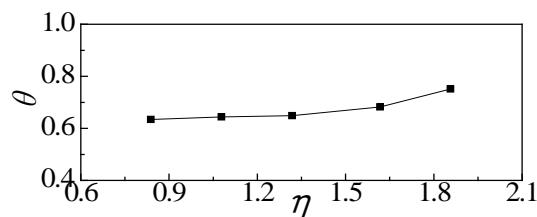
Fig.7 Relationship between θ and ρ_{st} (SCB10~ SCB14)
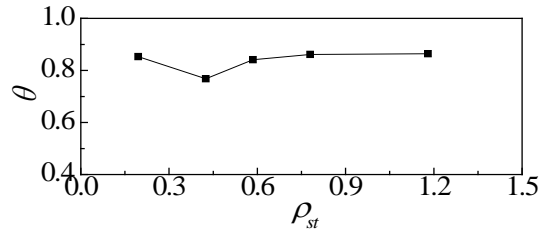
2.3.2 Effect of degree of shear connection on slip and deflection curves

Fig.8 shows slip comparison by test and FEA when $P/P_u=0.4$. The comparison between SCB1 and SCB2 demonstrates that: (1) The degrees of the shear connection have significant impact on the interface slip. The degree of shear connector of SCB1 is 0.85 and that of SCB2 is 0.34. The bigger the degree of shear connection, the smaller the interface slip. (2) The maximum slip is observed in 1/6 span from fulcrum. The slip of pure bending section is small because the shear force is zero under such condition; while the sliding of fulcrum is small owning to that the joints of concrete slab is constrained by support.

Fig.9 illustrates the deflections of the composite beams SCB1 and SCB2 under dynamic loading obtained by both test and FEA when $P/P_u=0.4$. The deflections of SCB1 are lower than those of SCB2, which demonstrates that the degree of shear connection could have significant impact on the deflection. The deflection is increased as the shear connection degree is decreased, that is, the bigger the shear connection degree, the larger the flexural stiffness.
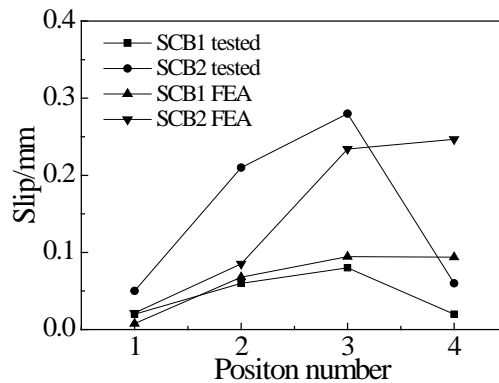

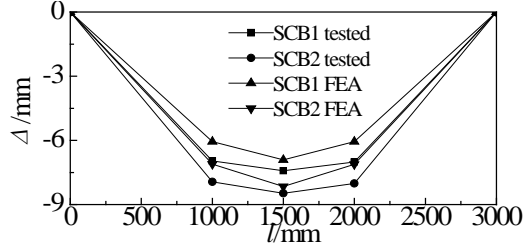Fig.8 Distribution of slip along span

Fig.9 Deflection of steel-concrete composite beam

3. Standard methods to estimate flexural stiffness

Degree of shear connection is an essential factor for the calculation of steel-concrete composite beams flexural stiffness in various codes, so its definition is presented here with the expression for the following analysis and discussion. After that, three widely used standard methods to estimate flexural stiffness are summarized below for comparison.

$$\eta = n/n_f \tag{2}$$

where n=actual number of shear connectors between intermediate point and the adjacent support. n_f = number of connectors for full shear connection. $n_f = V_s/V_u$. V_s is the compression force in concrete slab for fully composite beam, and V_u is the nominal strength of one stud shear connector. The definition of V_s and V_u may vary with the standards.

3.1 GB standard

In Chinese national standard (GB 50017-2003), the flexural stiffness (EI) of steel-concrete composite beams is expressed as follows:

$$\left(EI\right) = \frac{\left(E_s I_{tr}\right)}{1+\zeta} \tag{3}$$

$$\zeta = m\left[0.4 - \frac{3}{(jl)^2}\right], m = \frac{36E_s d_c p_1 A_0}{n_s V_u hjl^2}, j = 0.81\sqrt{\frac{n_s V_u A_1}{EI_0 p_1}}, A_0 = \frac{A_c A_s}{\alpha_E A_s + A_c}, A_1 = \frac{I_0 + A_0 d_c^2}{A_0}, I_0 = I_s + \frac{I_c}{\alpha_E}$$

where I_c=moment inertia of concrete, I_s=moment of inertia of steel section. d_c =distance between concrete neutral axis to steel beam neutral axis. h=depth of entire section. n_s=number of shear studs per row across flange. $\alpha_E = E_s/E_c$. A_c=area of concrete cross section, and A_s=area of steel cross section. The stud shear bearing capacity can be determined by:

$$V_u = 0.43A_{sd}(f_c E_c)^{0.5} \le 0.7A_{sd}f_u \tag{4}$$

Where A_{sd} =area of stud shear connector cross section. f_u=ultimate strength of stud. f_c=compressive strength of concrete. V_s is the smaller of $A_s f_s$ and $A_c f_c$.

9

3.2 AISC standard

In the AISC-LRFD commentary, the flexural stiffness of steel-concrete composite beams is given as:

$$(EI)=E_s\left[I_s+\eta^{0.5}\left(I_{tr}-I_s\right)\right] \tag{5}$$

where V_s is the smaller of A_sf_s and $0.85A_cf_c'$. The nominal strength of on stud shear connector embedded in solid concrete is:

$$V_u = 0.5A_{sd}(f_c'E_c)^{0.5} \leq A_{sd}f_u \tag{6}$$

where f_c'=compressive strength of concrete cylinders.

3.3 British standard

In the British standard BS5950-3.1 commentary, the deflection under service loads for partial shear connection should be determined by:

$$\delta = \delta_c + \beta(1-\eta)(\delta_s - \delta_c) \tag{7}$$

Where δ_c=deflection for the steel beam acting alone; δ_s=deflection of a composite beam with full shear connection for the same loading. For propped construction, β=0.3; for unpropped construction, β=0.5. V_u decided by the stud diameter and concrete compression. V_s is the smaller of A_sf_s and $0.45A_cf_{cu}$. According to the load-deflection curve transformation by Eq.(7), it can get the flexural stiffness of steel-concrete composite beams.

4. FE analysis

4.1 FE modeling degree of connection

4.1.1 Material constitutive models

The material constitutive models of concrete suggested by Ding *et al*.(2011) are used for the model.

$$y = \begin{cases} \dfrac{kx+(m-1)x^2}{1+(k-2)x+mx^2} & x \leq 1 \\ \dfrac{x}{\alpha_1(x-1)^2 + x} & x > 1 \end{cases} \tag{8}$$

where k is a ratio of the initial tangent modulus to the secant modulus at peak stress and equals to $9.1 f_{cu}^{-4/9}$. m is a parameter that controls the decrease in the elastic modulus along the ascending

portion of the axial stress-strain relationship and equals to $1.6(k-1)^2$. For a steel-concrete composite beam, parameter α_1 is determined by regression analysis as:$\alpha_1=2.5\times10^{-5}f_{cu}^3$.

The Poisson ratio v_c of concrete is taken as 0.2. Eq.(8) is able to describe the stress-strain relationship of concrete with strengths ranging from 20MPa to 140MPa which has been validated by experimental results (Ding *et al.* 2011).

An elasto-plastic model, with consideration of Von Mises yield criteria, Prandtl-Reuss flow rule, and isotropic strain hardening, is used to describe the constitutive behavior of steel. The expression for the stress-strain relationship of steel beam and rebar is as below (Ding *et al.*2011).

$$\sigma_i = \begin{cases} E_s\varepsilon_i & \varepsilon_i \leq \varepsilon_y \\ f_s & \varepsilon_y < \varepsilon_i \leq \varepsilon_{st} \\ f_s + \zeta E_s(\varepsilon_i - \varepsilon_{st}) & \varepsilon_{st} < \varepsilon_i \leq \varepsilon_u \\ f_u & \varepsilon_i > \varepsilon_u \end{cases} \tag{9}$$

where σ_i is the equivalent stress of steel; f_s is the yield strength; f_u is the ultimate strength and $f_u=$ $1.5f_s$; E_s is the elastic modulus, $E_s=2.06\times10^5$MPa; E_{st} is the strengthening modulus, which is described by $E_{st} = \zeta E_s$; ε_L is the equivalent strain; ε_y is the yield strain; ε_{st} is the strengthening strain; and ε_u is the ultimate strain, which is described by $\varepsilon_u =\varepsilon_{st} + 0.5 f_s /(\zeta E_s)$, where $\varepsilon_{st} = 12\varepsilon_y$, ε_u $=120\varepsilon_y$ and $\zeta = 1/216$.

The ideal elastic-plastic model was used for the studs in the concrete slabs, and the constitutive relation is as follows:

$$\sigma_{is} = \begin{cases} E_{ss}\varepsilon_{is} & \varepsilon_{is} \leq \varepsilon_{ys} \\ f_{ss}+0.01E_{ss}(\varepsilon_{is} - \varepsilon_{ys}) & \varepsilon_{ys} < \varepsilon_{is} \leq \varepsilon_{us} = 21\varepsilon_{ys} \\ f_{us} = 1.2f_{ss} & \varepsilon_{is} > \varepsilon_{us} \end{cases} \tag{10}$$

where σ_{is} is the equivalent stress of stud; f_{ss} is the yield strength; $f_{us}$is the ultimate strength and f_{us} $=1.2f_{ss}$; E_{ss} is the elastic modulus of stud as 2.06×10^5; ε_{is} is the equivalent strain, ε_{ys} is the yield strain and ε_{us} is ultimate strain of stud.

The stiffness of spring element is defined by load-slip curves and is used to simulate the shear stud. The well-known formula proposed by Ollgaard *et al.*1971 that has been widely used in the literature.

$$V/V_u=(1-e^{-0.71s})^{0.4} \tag{11}$$

where s is the average slip, V is shear capacity per stud. For a slip up to 5 mm, V reaches 99% of the ultimate load V_u. When the longitudinal, lateral and vertical stiffness adopt the expression (11) in this paper, nice results can be obtained.
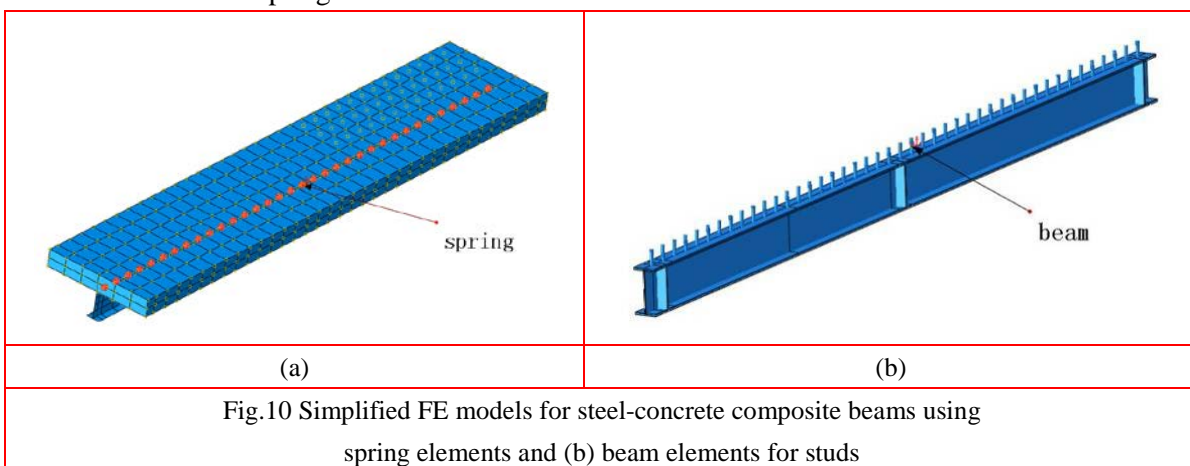
4.1.2 Model skills

FE models are established by ABAQUS program (Hibbitt 2003), which is extensively adopted to analyze the composite structures and rock structures (Chang *et al.* 2014; Chang *et al.*,

2015a; 2015b). Four-node reduced integral format shell elements (S4R) are employed to model the steel beams. Concrete are modeled by eight-node brick elements (C3D8R). Steel reinforcement bars in specimens are modeled by the truss element T3D2.

In the FE model shown in Fig.10(b), beam element (B31) is used to model the studs, and the studs are embedded in the concrete slab. The stiffness of the beam elements to represent the nonlinear load-slip relationship is then computed by ABAQUS.

The structured meshing technique is adopted. Mesh convergence studies are first performed to ensure that the FE mesh is sufficiently fine to give accurate results, and secondly, guarantee the computational efficiency. The selected meshed models used for modeling are shown in Fig.10. The type of contact between the steel and concrete is defined as surface to surface and coulomb friction model between concrete and steel is adopted for simulation. In the tangential direction, a friction coefficient of 0.5 is used for analysis. The sliding formulation is finite sliding, and a hard contact is defined in the normal direction. The boundary of the steel-concrete composite beam is simply supported as in the FE model.

Typical load-deflection curves of the specimens obtained from the FEA in comparison with the experimental results are shown in Fig.11. The curves of slips at beam end versus load are shown in Fig.12. Good agreement between experimental and FE modeling results are found in the elastic stage, and in the elastic-plastic stage and failure stage, the curve from FEA and the measured curve appeared with certain deviation. The simplified FE modeling approach using springs or beam elements can provide satisfactory modeling results for the experimental scenarios investigated. It can be seen from the results, the beam end slip obtained by using beam element method is smaller than that using the spring element model. This agrees with the bending stiffness obtained from load deflection curve. The bending stiffness obtained by using beam element method is larger than that using the spring element model. The consistent findings from the end slip and bending stiffness indicate that the beam element could provide stronger connection than the spring element.
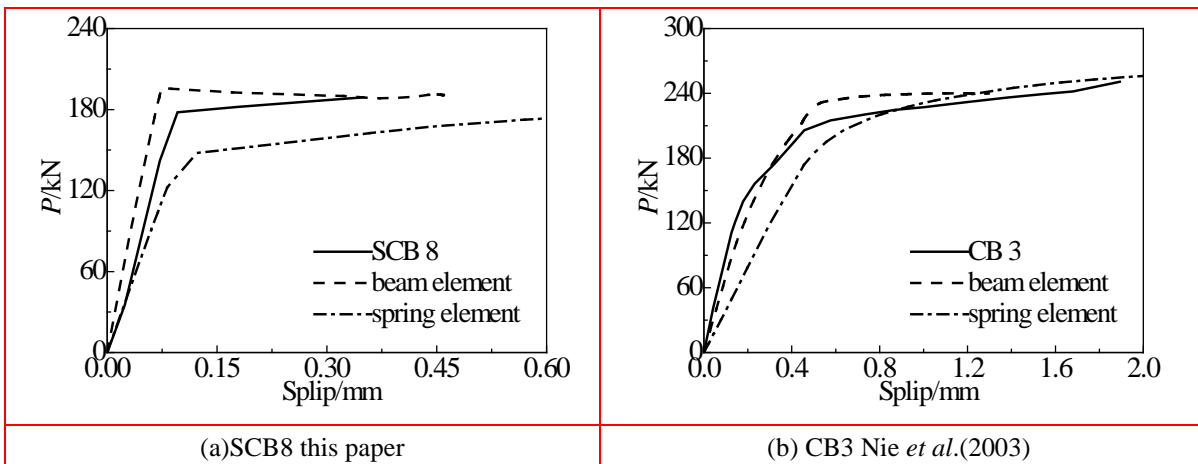

(a)	(b)

Fig.10 Simplified FE models for steel-concrete composite beams using spring elements and (b) beam elements for studs

(a)SCB8 this paper

(b)CB3 Nie *et al.*(2003)

(c)SCB1 zhao *et al.*(2012)

(d) B1 Souici *et al.*(2013)

Fig.11 Comparison between calculated and tested ones on load-deformation
of steel-concrete composite beam

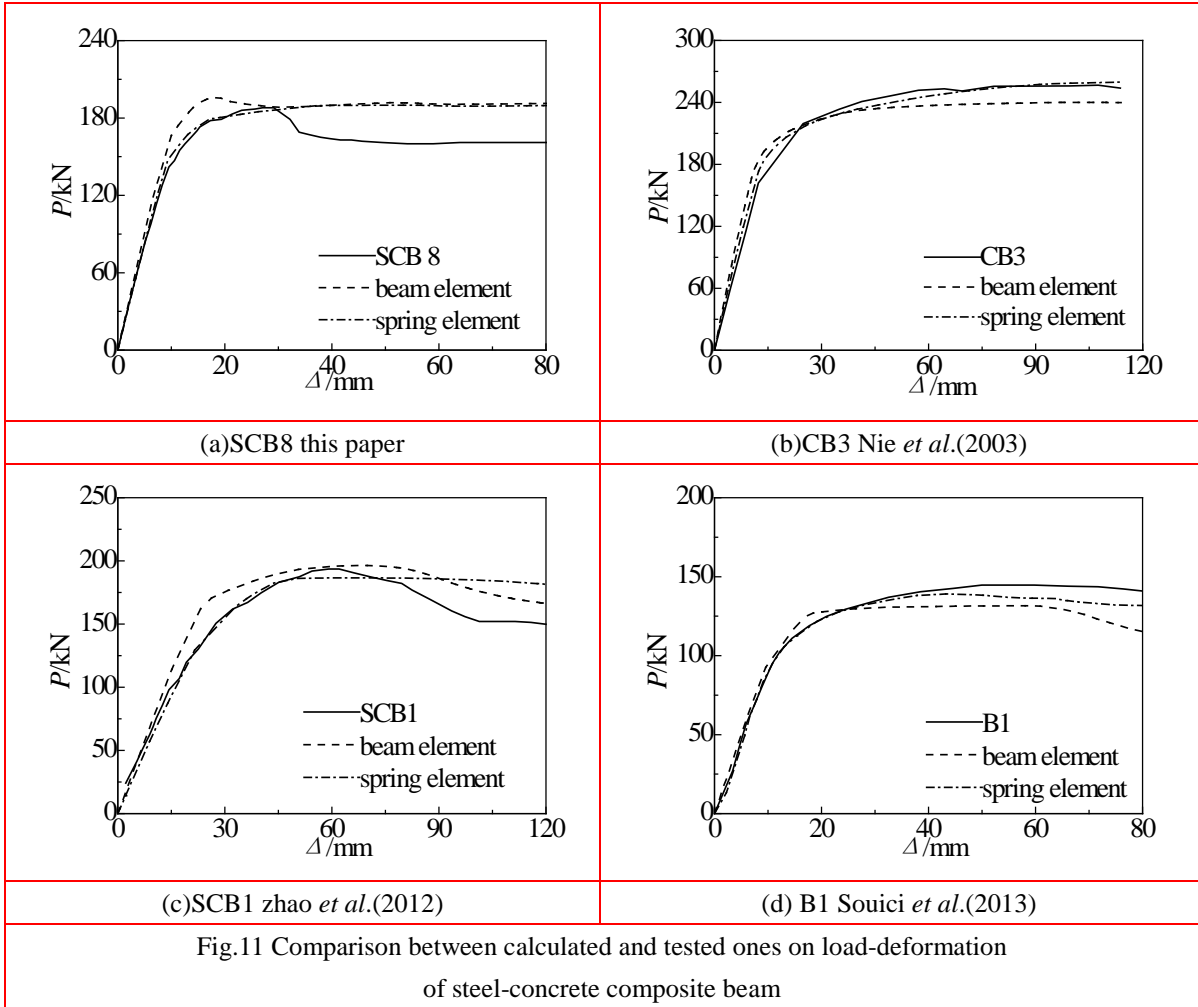(a)SCB8 this paper

(b) CB3 Nie *et al.*(2003)

Fig.11 Comparison between calculated and tested ones on load-end slip of composite steel-concrete beam of steel-concrete composite beam

4.2 Flexural stiffness from FEA

For FEA, 19 groups of experimental data on steel-concrete composite beams are included for model validation and analysis. The longitudinal reinforcement is considered when computing the flexural stiffness of composite beams.

(EI) is the measured values of flexural stiffness, $(EI)_{11}$ is the flexural stiffness by spring element computing method. $(EI)_{12}$ is the flexural stiffness by beam element computing method. $(EI)_2$ is the flexural stiffness by Eq.(3). $(EI)_3$ is the flexural stiffness by Eq.(5). $(EI)_4$ is the flexural stiffness by Eq.(7). The experimental results are compared with the predicted results using different methods including FEA, Eqs.(3), (5), and (7).

Table 3 shows comparison between simulated results and test results of steel-concrete composite beam. The average $(EI)/(EI)_{11}$ ratio is 1.003 with a coefficient of variation at 0.079 for spring element. The average $(EI)/(EI)_{12}$ ratio is 0.962 with a coefficient of variation at 0.084 for beam element. Such findings indicate that the FE simulation results are very close to the experimental results. Table 1 illustrates comparison all test data with equations in different design codes.

The average $(EI)/(EI)_2$ ratio is 0.939 with a coefficient of variation at 0.250 for Eq.(3). The average $(EI)/(EI)_3$ ratio is 0.747, and average $(EI)/(EI)_3$ ratio is 0.763. The results of Eq.(5) and Eq.(7) are larger and more conservative than the test results. This is because the degrees of shear connection of the majority specimen are greater than 1, however, both AISC-LRFD and BS5950-3.1do not consider the slip between concrete slab and steel beam. Therefore, there is no reduction coefficient considered for flexural stiffness. That is why both standards give larger values.

Taking SCB3~SCB7 specimens with varied stud spacing as examples, the relationship between θ and η obtained from each standard in comparison to that from test results is presented in Fig.13, respectively. (1) It should be noticed that the different definition about the degree of shear connection in different standards caused the variance of η value. (2) When η is greater than 1, the results from both Eqs.(5) and (7) agree well with the transformed section method. When η is less than 1, results from Eqs.(5) and (7) are different. (3) when the degree of shear connection is less than 0.5, Eq.(3) could give an abnormal flexural stiffness coefficient. When the degree of shear connection is greater than 1, Eq.(3) still considers a reduction factor and the value from this equation is smaller than the measured values.
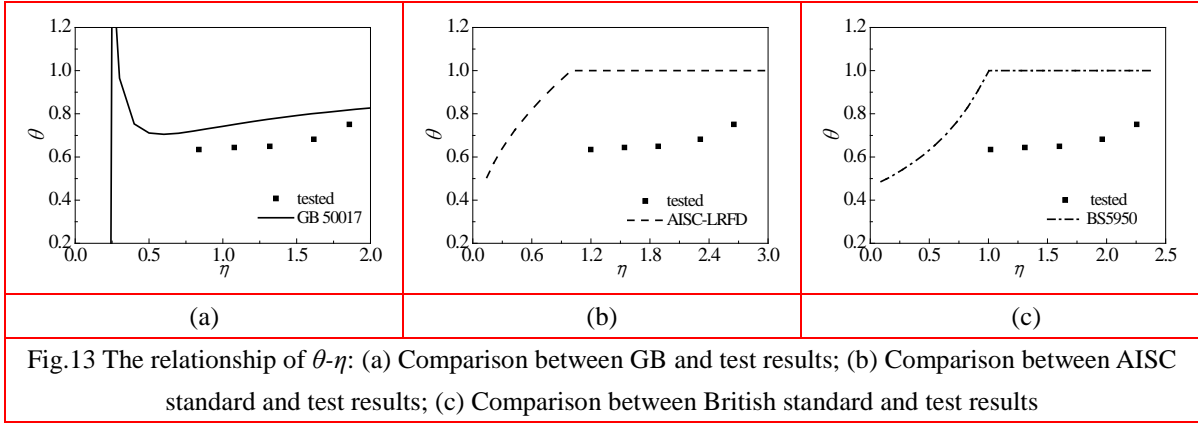
Fig.13 The relationship of θ-η: (a) Comparison between GB and test results; (b) Comparison between AISC standard and test results; (c) Comparison between British standard and test results

Table 3 Comparison between calculated and tested ones of composite steel-concrete beam

No.	Source of the specimens	Total number of specimens	Characteristic value	spring element	Beam element	Eq.(3)	Eq.(5)	Eq.(7)
				$(EI)/(EI)_{11}$	$(EI)/(EI)_{12}$	$(EI)/(EI)_2$	$(EI)/(EI)_3$	$(EI)/(EI)_4$
1	this paper	14	Average	0.997	0.956	0.941	0.762	0.785
			Coefficient of variation	0.069	0.088	0.301	0.162	0.245
2	Nie et al.(2003)	4	Average	0.928	0.909	0.841	0.641	0.641
			Coefficient of variation	0.100	0.090	0.075	0.151	0.151
3	Salari (1999)	1	Average	1.080	0.995	1.211	0.867	0.867
			Coefficient of variation	/	/	/	/	/
4	Zhao et al. (2012)	2	Average	1.084	0.978	0.807	0.641	0.641
			Coefficient of variation	0.021	0.011	0.057	0.009	0.009
5	Souici et al. (2013)	3	Average	1.052	1.035	1.056	0.846	0.870
			Coefficient of variation	0.052	0.064	0.095	0.160	0.143
	All above	24	Average	1.003	0.962	0.939	0.747	0.763
			Coefficient of variation	0.079	0.084	0.250	0.172	0.225

4.3 Parametric study

It can be seen that the FE models can accurately simulate the flexural stiffness for the

steel-concrete composite beams from section 4.2. In this section, parametric studies are conducted to investigate the dominant factors on the flexural stiffness. In addition, comparison study is also conducted between the FEA results and the standard results. Spring element is used for FEA in the following study with the reasons addressed as follows. Firstly, spring element can increase the computing efficiency for FEA. Secondly, spring element can simulate the stud stiffness value accurately in each direction, which is important for the simulation as the stud stiffness reflects the stud mechanical properties on the steel-concrete composite beams under positive bending.

4.3.1 Influence of shear connection degree

Fig.14 shows the geometric properties of steel-concrete composite beam, which loaded in mid-span, steel-concrete composite beam depth-span ratio, beam size, concrete wing size values are according to specification GB 50017-2003.2003. For convenient analysis, there is no longitudinal reinforcement in concrete slab. The span is 12 m. The stud is arranged in a single row layout, the stud diameter is 19 mm and its yield strength and ultimate strength are 350 MPa and 455 MPa respectively. There are 6 types of material combination groups in total for steel-concrete composite beam models: (1) Q235 steel paired with C30 and C40 concrete, (2) Q3455 steel paired with C40 and C50 concrete, (3) Q420 steel paired with C50 and C60 concrete. In total there are 43 cases for study. Fig.15 shows θ-η relationship of steel-concrete composite beams under different degree of shear connection. Relationships between θ and η for Q345 matching C40 example are also obtained from three different codes and compared with the FEA results.
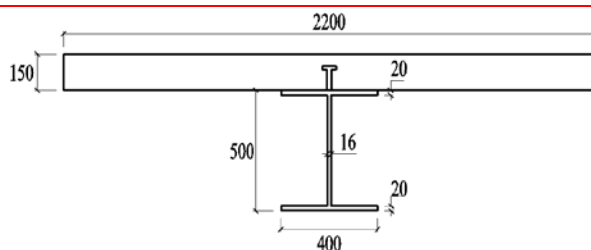

Fig.14 Geometric properties of steel-concrete composite beam

4.3.2 Influence of other factors

Fig.15 shows the η-θ relationship in 43 groups steel-concrete composite beams. It is found that, the shear connection degree has significant impact on flexural stiffness coefficient of steel-concrete composite beams. θ is increased with the increase of η value, but this phenomenon is not obvious when the connection degrees is more than 1.

(1) Stud in double row layout

In this investigation, stud yield strength and ultimate strength, beam size and span, and stud diameter are the same as those defined in Section 4.1. In this analysis, two groups of composite beams are studied, with one group using Q235 steel and C30 concrete and the other using Q420

steel and C50 concrete. Fig.16 demonstrates the relationship between η and θ when stud is arranged in a double row layout. It can be seen that, the double row stud arrangement has little influence on flexural stiffness coefficient of steel-concrete composite beams. θ-η relationship of composite beam with Q235 steel and C30 concrete obtained from GB, AISC, and British standard are also presented in Fig.16, respectively in comparison to the FEA results..

(2) The diameter of stud

In this investigation, stud yield strength and ultimate strength, beam size and span, and number of shear studs per row across flange are the same as those defined in Section 4.1 In this analysis, two groups of composite beams are studied, with one group using Q235 steel and C30 concrete and the other using Q420 steel and C50 concrete. The stud diameter are 16 mm, 22 mm, 25 mm respectively. Fig.17 illustrates the relationship between η and θ. It can be found that, diameter of stud has little influence on flexural stiffness coefficient of steel-concrete composite beams. θ-η relationship of composite beam with Q235 steel and C30 concrete obtained from GB, AISC, and British standard are also presented in Fig.17, respectively in comparison to the FEA results.

(3) The loading position and way

In this investigation, stud yield strength and ultimate strength and beam size, and the diameter of stud are the same as those defined in Section 4.1. In this analysis, two groups of composite beams are studied, with one group using Q235 steel and C30 concrete and the other using Q420 steel and C50 concrete. The concentrate loading position are 1/4, 1/3, 5/12 of beam span, and uniformly distributed loading is also adopted. Fig.18 shows the relationship between η and θ, it is found that, the loading position and way has few influence on flexural stiffness coefficient of steel-concrete composite beams. θ-η relationship of composite beam with Q235 steel and C30 concrete obtained from GB, AISC, and British standard are also presented in Fig.18, respectively in comparison to the FEA results.

(4) Span

In this investigation, stud yield strength and ultimate strength, beam size and span, and the diameter of stud are the same as those defined in Section 4.1. In this analysis, two groups of composite beams are studied, with one group using Q235 steel and C30 concrete and the other using Q345 steel and C40 concrete. The span are 4 m, 8 m,16 m, 20 m respectively. Fig.19(a)~(d) shows the relationship between η and θ. It is found that, the beam span has some influence on flexural stiffness coefficient of steel-concrete composite beams, it is because in this analysis, when the span is bigger, the ratio of flexural stiffness of steel girder to composite beam is larger, so θ increased as the span increased. θ-η relationship of composite beam with Q345 steel and C40 concrete obtained from GB, AISC, and British standard are also presented in Fig.19 respectively in comparison to the FEA results.

The parameters of steel concrete composite beam considered in the parametric study include :

concrete strength from C30 to C60, steel strength from Q235 to Q420, stud row layout - single or double, stud diameter from 16 mm to 25 mm, stud yield strength and ultimate strength - 350 MPa and 455 MPa respectively, beam span from 4 m to 20 m, shear span ratio from 1/4 to 1/2, load ways including point loading and uniformly distributed loading. The overall geometry of specimens in this parametric investigation, namely the geometry of concrete slab, steel beam, headed studs, and strength of materials, is shown in Table 4.
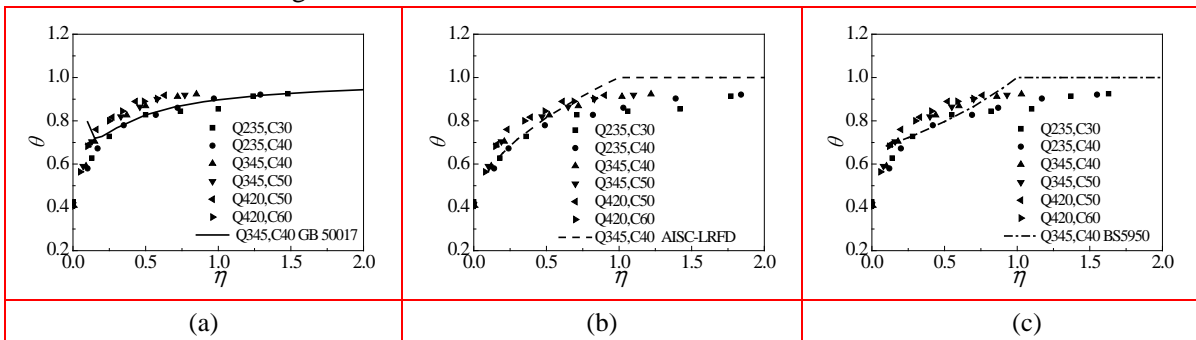

| (a) | (b) | (c) |

Fig.15 The relationship of θ-η : (a) Comparison between GB standard and FEA results; (b) Comparison between AISC standard and FEA results; (c) Comparison between British standard and FEA results

| (a) | (b) | (c) |

Fig.16 Influence of double row stud to relationship of θ-η (a) Comparison between GB standard and FEA results; (b) Comparison between AISC standard and FEA results; (c) Comparison between British standard and FEA results
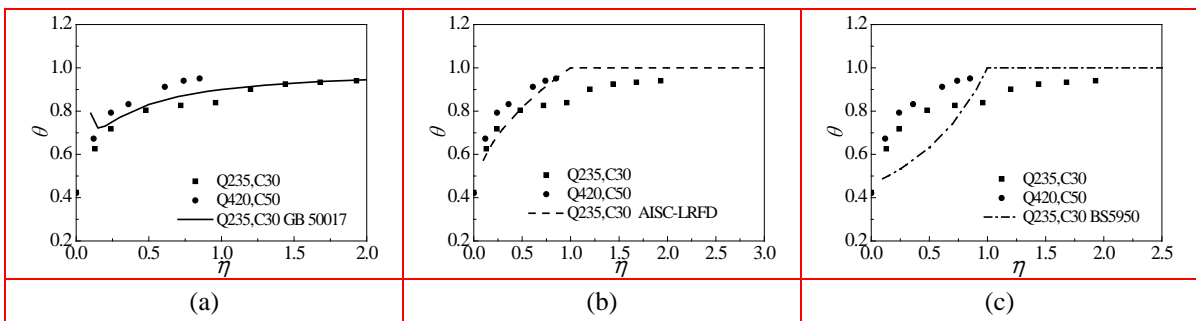

| (a) | (b) | (c) |

Fig.17 Influence of stud diameter to relationship of θ-η (a) Comparison between GB standard and FEA

Fig.18 Influence of loading position and model to relationship of *θ-η* (a) Comparison between GB standard and FEA results; (b) Comparison between AISC standard and FEA results; (c) Comparison between British standard and FEA results
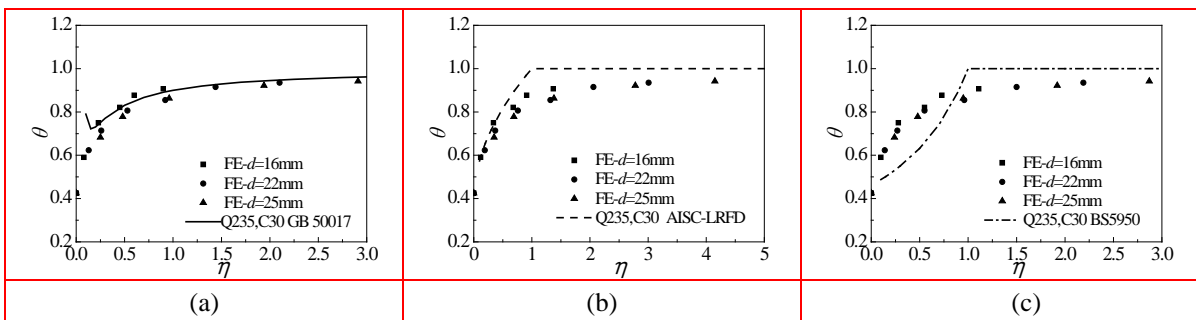

(a)

(b)
(1)*l*=4m

(c)

(a)

(b)
(2)*l*=8m

(c)

(a)	(b) (3)*l*=16m	(c)
(a)	(b) (4)*l*=20m	(c)

Fig.19 Influence of beam length to relationship of θ-η (a) Comparison between GB standard and FEA results; (b) Comparison between AISC standard and FEA results; (c) Comparison between British standard and FEA results
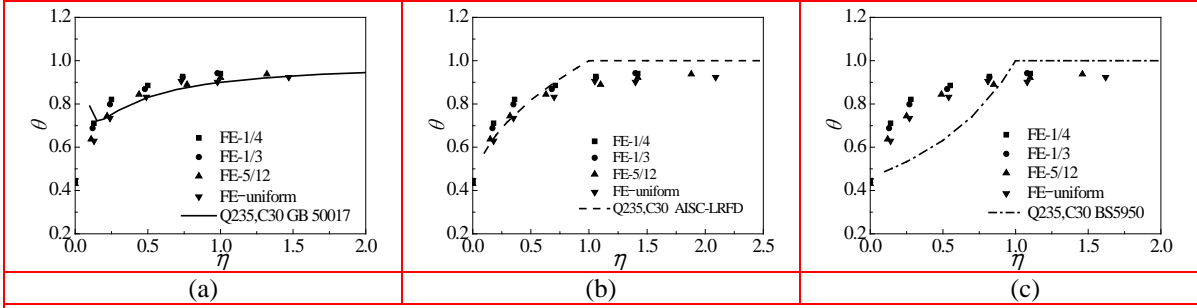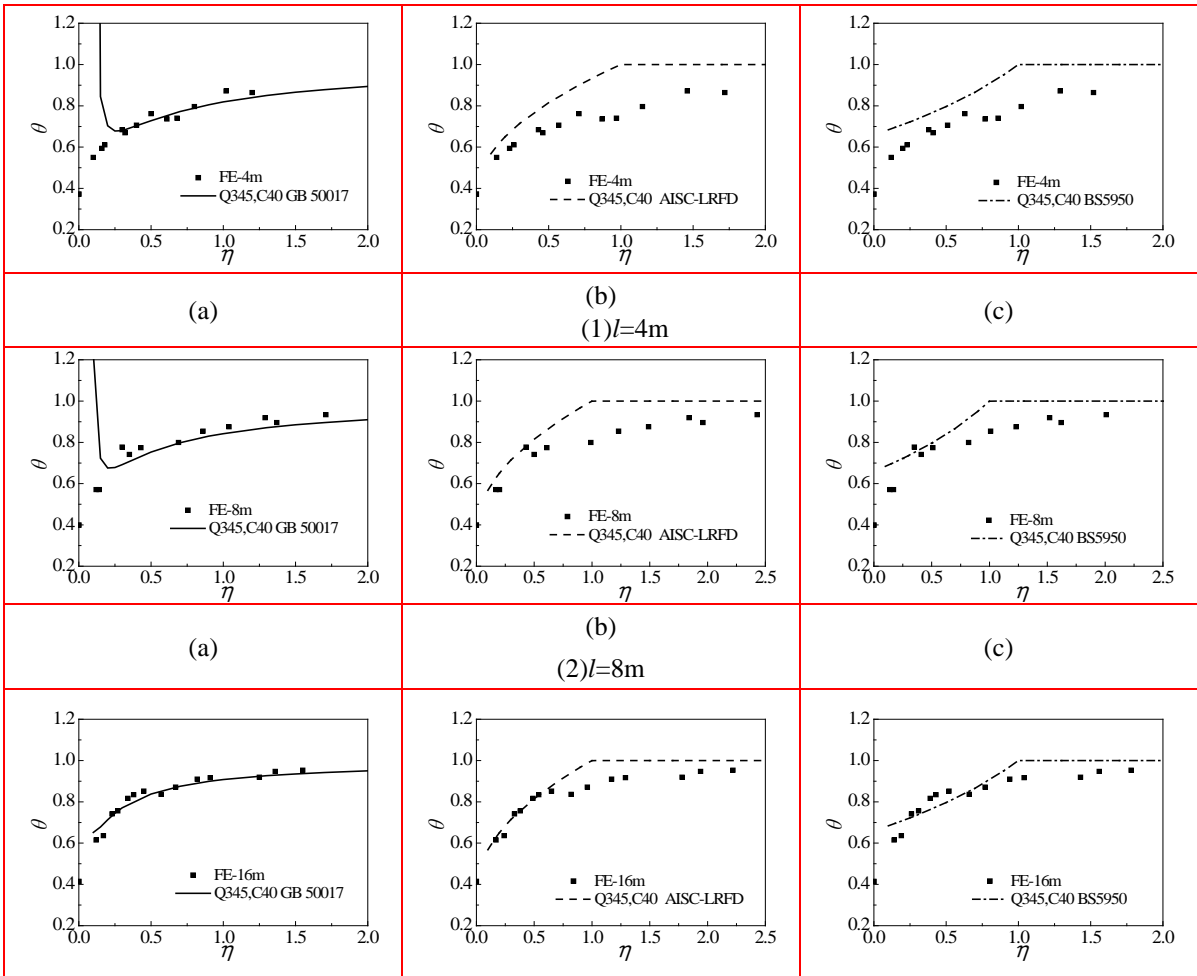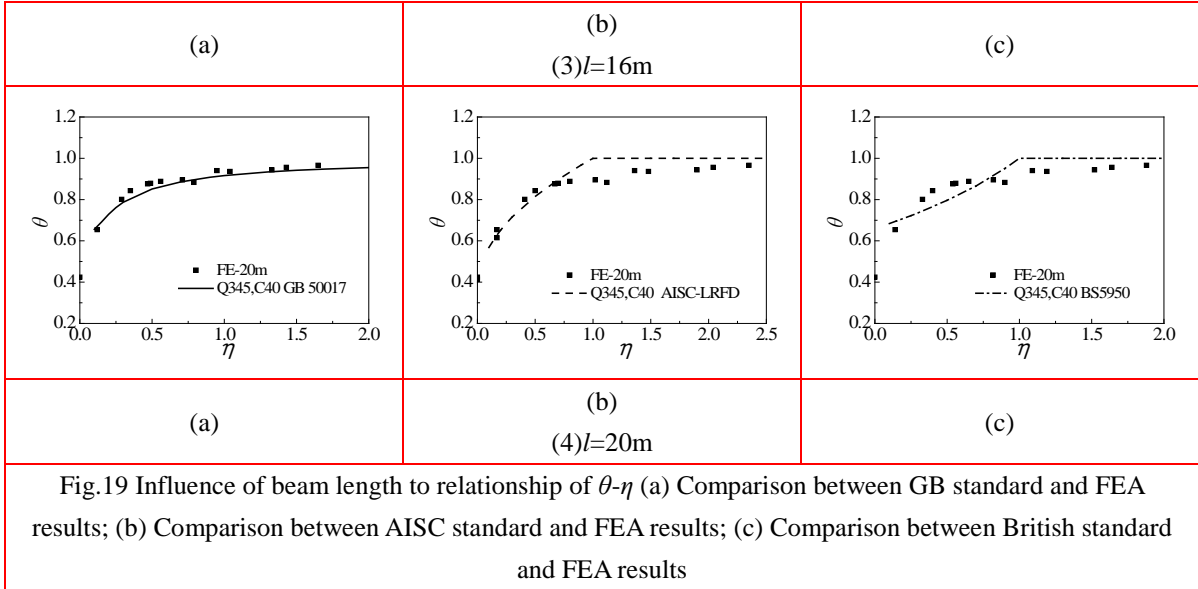
Table 4 Parameters of composite steel-concrete beam

l/m	h_c /m	b_c/m	h_s /m	b_s/m	d /mm	f_s /MPa	f_u/MPa	f_{cu}/MPa	f_y/MPa
4	0.08	0.8	0.2	0.1	16	350	455	C40	235,345
8	0.12	1.5	0.4	0.25	16	350	455	C40	235,345
12	0.15	2.2	0.5	0.4	19	350	455	C30,C40, C50,C60	235,345,420
16	0.16	2.4	0.75	0.45	19	350	455	C40	235,345
20	0.2	2.6	0.9	0.5	22	350	455	C40	235,345

4.3.3 Summary and discussion

Figs.15~19 show that: (1) When the shear connection degree is greater than 0.5, results according to GB 50017-2003 is in good agreement with the FEA results. When the shear connection degree is less than 0.5, and span of beam is less than 12 m, flexural stiffness coefficient appear abnormal phenomenon. (2) Results from AISC-LRFD and BS5950-3.1 are different from the FEA results, and the results from the codes are mostly on the larger side.

FEA results by ABAQUS are compared with formula (3) (5) (7), as shown in Table 5. The shear connection degree is generally greater than 0.5 in practice, therefore the connection degree greater than 0.5 is considered in the validation. In Table 5, $(EI)_{FE}$ is the measured values of flexural stiffness by ABAQUS.

The average $(EI)_{FE}/(EI)_2$ ratio is 1.024 with a coefficient of variation at 0.024. The average $(EI)_{FE}/(EI)_3$ ratio is 0.924 with a coefficient of variation at 0.065. The average $(EI)_{FE}/(EI)_4$ ratio is 0.952 with a coefficient of variation at 0.078. Therefore, in general, in predicting the flexural stiffness of steel-concrete composite beam, Eq.(3) provided higher accurate results with small

coefficients of variation values than Eq.(5) and Eq.(7).

With both experimental research and FEA, Fig.19 (1)~(4) shows that when the span is small (l=4, 8m), GB 50017-2003 may provide abnormal stiffness values. That is because in Eq.(3), when l is little and p_1 is large, ζ will be very small, which leads $1/(1+\zeta)$ value to an extremely large value.

Table 5 Comparison between Eqs.(3) (5) (7) results and FE ones

No.	Type	Total number of specimens	Characteristic value	Eq.(3) $(EI)_{FE}/(EI)_2$	Eq.(5) $(EI)_{FE}/(EI)_3$	Eq.(7) $(EI)_{FE}/(EI)_4$
1	Material	43	Average	1.023	0.941	0.980
			Coefficient of variation	0.013	0.060	0.076
2	Row of stud	17	Average	1.017	0.940	0.915
			Coefficient of variation	0.020	0.091	0.115
3	Diameter of stud	19	Average	1.020	0.914	0.940
			Coefficient of variation	0.028	0.047	0.048
4	Load pattern	26	Average	1.052	0.930	0.988
			Coefficient of variation	0.017	0.026	0.062
5	Span	57	Average	1.017	0.909	0.935
			Coefficient of variation	0.025	0.071	0.070
6	Total	162	Average	1.024	0.924	0.952
			Coefficient of variation	0.024	0.065	0.078

5. Conclusions

From this study, the following conclusions can be drawn.

(1) The experimental results suggest that the bigger the connection degree is, the larger the flexural stiffness will be.

(2) Both beam element and spring element could be used to model the stud. Both element methods achieved good agreement with the test results. However, in comparison, the spring element method has higher accuracy and faster computational speed than beam element method.

(3) Based on parametric analysis with spring element, it is found η is the main factor influencing the flexural stiffness coefficient. The greater the degree of shear connection, the larger the flexural rigidity coefficient of composite beams. However, after the degree of shear connection reaching 1, the growth of flexural stiffness coefficient is not significant. Other factors including stud in double row layout, stud diameter, beam span, loading location and way, had little impact on the flexural stiffness.

(4) When the shear connection degree is greater than 0.5, the flexural stiffness given by GB

50017-2003 is in good agreement with that from FEA. The flexural stiffness obtained from AISC-LRFD and BS5950-3.1 is generally larger than that obtained from the FEA results. The results indicate that GB 50017-2003 may provide a better estimation in comparison to the other two standard methods.

Acknowledgment

Refrences

AISC-LRFD. (2005), *Load and resistance factor design specification for structural steel buildings*, 2nd ed. American Institute of Steel Construction (AISC), Chicago, US.

BS5950-3.1: British Standard,(1990), *Structural use of steelwork in building*. Par3: Design In Composite Construction. British Standards Institution, London, UK.

Chang, X., Luo, X.L., Zhu, C.X. and Tang, C.A. (2014), "Analysis of circular concrete-filled steel tube support in high ground stress conditions". *Tunn. Undergr. Sp. Tech.*, **43**(3), 41-48.

Chang, X., Wang, J.H, Zhang, Z.H. and Tang, C.A. (2015a), "Effects of interface behavior on fracture spacing in layered rock". *Rock Mech. Rock Eng.*, 48:1-14.

Chang, X., Shan, Y.F, Zhang, Z.H, Tang, C.A. and Ru, Z.L. (2015b), "Behavior of propagating fracture at bedding interface in layered rocks". *Eng. Geol.*, **197**(10):33-41

Dias M M, Tamayo J L P and Morsch I B. (2015), "Time dependent finite element analysis of steel-concrete composite beams considering partial interaction". *Computers & Concrete*, **15**(4):687-707.

Ding, F.X., Ying, X.Y., Zhou, L.C. and Yu, Z.W. (2011), "Unified calculation method and its application in determining the uniaxial mechanical properties of concrete ". *Front. Archit. Civ. Eng. China*. **5**(3), 381-393.

Ding, F.X., Liu, J., and Liu, X.M. (2015), "Mechanical behavior of circular and square concrete filled steel tube stub columns under local compression". *Thin Wall Struct.*, 2015, 94(9): 155-166.

Ding, F.X., Fu, L. and Liu, X.M. (2016a), "Mechanical performances of track-shaped rebar stiffened concrete-filled steel tubular (SCFRT) stub columns under axial compression", *Thin Wall Struct.*, **99**(2): 168-181.

Ding, F.X., Lu, D.R. and Bai, Y. (2016b), "Comparative study of square stirrup-confined concrete-filled steel tubular stub columns under axial loading", *Thin Wall Struct.*, **98**(1): 443-453.

Eurocode 4, European Standard. (2004), *Design of composite steel and concrete structures*, Part

1.1: General rules and rules for buildings-General rules, EN 1994-1-1.

GB 50017-2003, China Standard. (2003), *Code for design of steel structures*. China Planning Press , Beijing, China.

Hou Z.M., Xia H. and Wang Y.Q. (2015), "Dynamic analysis and model test on steel-concrete composite beams under moving loads", *Steel.Compos.Struc.*, **18**(3):565-582.

Hibbitt, Karlson & Sorensen Inc. (2003), ABAQUS/standard User's Manual, Version 6.4.1., Pawtucket, RI, USA.

Lezgy-Nazargah and M, Kafi L. (2015), "Analysis of composite steel-concrete beams using a refined high-order beam theory". *Steel.Compos.Struc.*, **18**(6): 1353-1368.

Mirza, O. and Uy, B. (2011), "Behaviour of composite beam–column flush end-plate connections subjected to low-probability, high-consequence loading". *Eng.Struct.*, **33**(2),647-662.

Nie, J.G. and Cai, C.S. (2003), "Steel-concrete composite beams considering shear slip effects" „*J.Struct.Eng.*, **129**(4),495-506.

Nie, J.G., Tao M.X. and Cai, C.S. (2011), "Analytical and numerical modeling of prestressed continuous steel-concrete composite beams". *J.Struct.Eng.*,**137**(12), 1405-1418.

Mohammad, R.S. (1999), "Modeling of bond-slip in steel-concrete composite beams and reinforcing bars ". Ph.D. Dissertation, University of Colorado, Colorado.

Kim, S.H., Jung, C.Y. and Ahn, J.H. (2011), "Ultimate strength of composite structure with different degrees of shear connection". *Steel.Compos.Struc.*, **11**(2), 375-390.

Ollgaard J G, Roger, G.S. and John, W.F. (1971), "Shear strength of stud connectors in lightweight and normal-weight concrete". *AISC Engineering Journal*, **8**(2),55-64.

Selçuk, E.G. and Metin, H. (2013), "Ultimate behavior of composite beams with shallow I-sections". *Steel.Compos.Struc.*, **14**(5), 493-509.

Souici, A., Berthet, J.F., Li, A. and Rahal, N. (2013), "Behaviour of both mechanically connected and bonded steel-concrete composite beams". *Eng.Stuct.*, **49**(4), 11-23.

Zhao, H.L., Yu, Y. and Ye. Z.M., (2012), "Simplified nonlinear simulation of steel-concrete composite beams". *J.Constr.Steel Res.*, **71**(4), 83-91.